Material swelling as the first step in the ablation of metals by ultrashort laser pulses

Juha-Matti Savolainen, Martin S. Christensen, and Peter Balling*
Department of Physics and Astronomy, Aarhus University, Ny Munkegade 120, DK-8000 Aarhus C, Denmark
(Received 2 September 2011; published 28 November 2011)

The ablation from a single-crystal Al(111) surface with single ultrashort near-infrared laser pulses has been investigated under ultrahigh vacuum conditions. Scanning-electron and atomic-force microscopy of the irradiated surface reveal a surprising development of the material response at increasing fluence: at low fluence, swelling exceeding one hundred nanometers dominates. At higher fluences, a hole is gradually formed in the swollen material, which eventually reaches below the original surface level. The observations indicate the significance of mechanical effects during ablation.

DOI: 10.1103/PhysRevB.84.193410 PACS number(s): 79.20.Eb, 61.80.Ba

Ultrashort-pulse excitation of solid materials has provided significant new information about the dynamics of highly excited matter. For instance, time-resolved x-ray diffraction experiments have shown how transient states of matter allow "ultrafast melting" of semiconductors (for a review, see Ref. 1). For metals, time-resolved electron diffraction experiments of thin aluminum foils have shown atomic disordering on a time scale of a few picoseconds.[2] The improved understanding of light–matter interaction has, ever since the first investigations of femtosecond-laser excitation, been paired with discussions about the possibilities of employing ultrashort-pulse laser excitation for precision manufacturing with minimized heat effects.[3–6] For further discussions about laser processing, please see Ref. 7.

Ultrashort-pulse excitation of bulk metals is normally described using the two-temperature model,[8] which has provided a good explanation of observations in the low-fluence regime of relevance for surface-chemical reactions,[9] and with appropriate modifications also in the fluence regime of relevance for modifications of the native material, e.g., by laser ablation.[10–15] The precise response of the metal samples to the high excitation is a topic of ongoing discussion, see Ref. 16 and references therein. In a thermal description, the material is rapidly heated, leaving an overheated liquid, which cools adiabatically and is expelled by evaporation, spallation or—in case the thermodynamic path takes the system close to the critical point—by phase explosion.

In this Brief Report, we report the surprising observation that the initial damage of a single-crystal metal surface induced by short-pulse excitation is not associated with significant material removal, rather with a pronounced swelling of the sample. As discussed in detail below, this observation is indicative of the strong mechanical effects that have been suggested to play a role during laser excitation. However, in contrast to predictions by molecular-dynamics simulations of the material response, significant material spallation does not set in immediately, rather a thick layer of material resolidifies in a foamy state with holes and voids, leaving a bump, which extends above the original surface level.

Prior to any investigations of the single-crystal Al (111) surface, it is cleaned by a sputter gun with 1 keV Ar^+ ions for 60 minutes. The Ar atoms are supplied by backfilling the UHV chamber to an Ar pressure of 3×10^{-5} torr. To eliminate possible defects introduced during the sputter process, the sample is subsequently annealed at 400 °C for 45 minutes. Multiple sputtering and annealing cycles are performed to remove the native 3–5 nm oxide layer and to assure a smooth surface.[17]

After preparation, the sample is exposed to a single 100-fs laser pulse with a central wavelength of 800 nm focused by a 25-cm achromatic lens. Pulse energies up to 800 μJ are available and the energy of each pulse is measured by a calibrated photo diode. Using a manual xyz stage and a vision system, the sample is translated by several beam diameters between each laser pulse. Figure 1 shows representative scanning electron microscopy (SEM) images of the irradiated spots for increasing fluences above the threshold for ablation. All images show a crownlike rim, or boundary, which increases in size as a function of the fluence. The two diameters of the axes of this elliptic feature, D_i (with i = major or minor), as a function of the pulse energy E_p follow to a good approximation the behavior $D_i^2 = 2\omega_i^2 \ln[2E_p/(\pi\omega_{\text{major}}\omega_{\text{minor}}F_{\text{th}})]$, which is expected for phenomena excited by a Gaussian beam exhibiting a well-defined threshold fluence, F_{th}.[18] A fit to the data (not shown) provides the laser spot sizes of the elliptic focus, $\omega_{\text{minor}} = (19 \pm 2)$ μm and $\omega_{\text{major}} = (25 \pm 2)$ μm (including an estimate of systematic errors), which agree well with the $\sim$20 μm calculated from the Gaussian parameters of the laser beam measured by a charge-coupled device (CCD) camera. The associated threshold fluence is (0.88 ± 0.09) J/cm^2. A threshold fluence determined in this way would often be coined an ablation threshold. However, atomic-force microscopy (AFM) images reveal that the situation is not that simple.

Figure 2 shows line outs obtained from AFM images of the laser-induced features for different fluences. It is apparent that the structures are not simple holes, rather bumps extending more than hundred nanometers above the original surface level. The topmost line out actually corresponds to a fluence, which is below the threshold for formation of the ring structure, which is clearly visible in Fig. 1. At gradually higher fluences, the ring can also be seen on the AFM line outs, since a hole is formed in the middle of the bump. It is, however, only at fairly high fluences that the hole extends below the original surface level.

In order to quantify this behavior, the hole depth is determined in a consistent manner by measuring the maximum depth in the middle of the ablation spot relative to the surrounding nondamaged surface. Single peaks due to surface

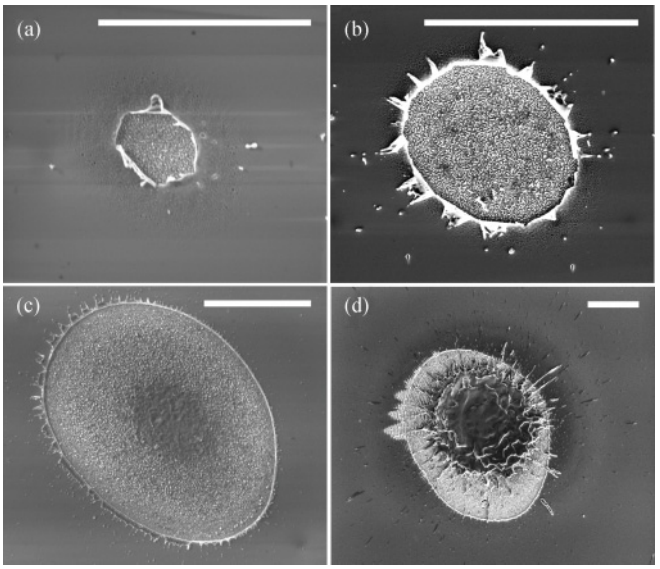

FIG. 1. Series of SEM images with increasing fluence. The white bars are 20 μm. Fluence in J/cm^2 are (a) 0.95, (b) 1.07, (c) 6.4, and (d) 30.

roughness in the height profiles are neglected. For the bumps, we measure the maximum height using the same criterion, and consider it as negative depth.

Figure 3 shows the measured "depth" as a function of fluence. The positive-depth data show signs of a logarithmic growth close to the threshold. This is the expected behavior if the energy is deposited exponentially into the sample and ablation occurs down to a depth where the energy density exceeds a certain threshold. Although it is by no means obvious that this model will capture the real ablation dynamics, Fig. 3 shows a logarithmic fit (dashed blue line) corresponding to an effective penetration depth of ~67 nm and a threshold of ~1.1 J/cm^2.

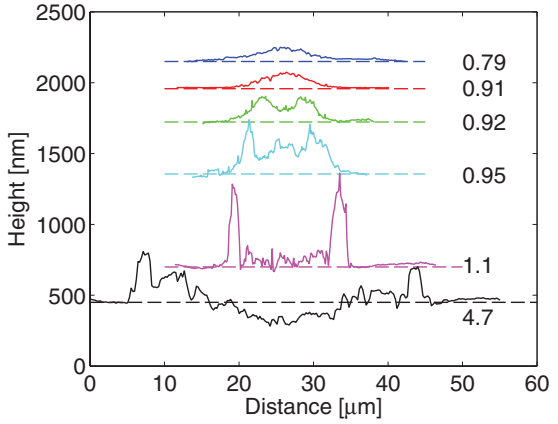

FIG. 2. (Color online) Examples of AFM line outs showing the evolution from bump to a deep hole for increasing single-shot fluences. Curves are labeled according to the fluence in J/cm^2. Note that curves have been vertically offset for clarity; the dashed lines represent the original surface level. The rim height in the 1.1 J/cm^2 curve is exaggerated due to an AFM-imaging artifact.

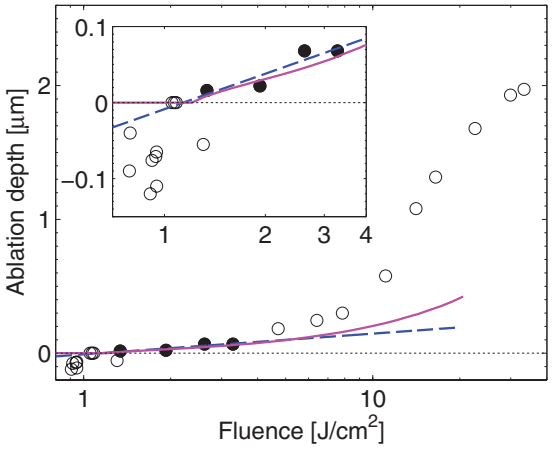

FIG. 3. (Color online) Ablation depth vs laser fluence. The dashed blue line shows a logarithmic fit to the data near threshold (filled circles), while the simulated depth is shown by a magenta solid line. The insert shows a blowup of the threshold region.

In a first attempt to model the observed phenomena, we have solved the two-temperature equations numerically and determine the ablation depth from the standard energy-density criterion, see Ref. 15 for details. Note that this model will not be able to capture the swelling, so we may only hope to compare to the positive depths. In the present simulation, we use the heat capacity given by the Sommerfeld theory, as it agrees well with the one calculated directly from the density of states.[19] Maybe somewhat surprisingly, there is both qualitative and quantitative agreement between the simulation and the experimental data in the low-fluence regime: the threshold and penetration depth from the simulation are 1.13 J/cm^2 and 54.3 nm, respectively, where the Fresnel reflectivity (0.869) has been used to convert incoming laser fluence to absorbed fluence.

In the high-fluence regime, above 4 J/cm^2, the experimentally determined depths are much larger than the simulation. This discrepancy may readily be attributed to a break down of the approximations behind the simulation. In this fluence regime, the morphology of the holes is gradually changing, exhibiting a flat central area and eventually signatures of violent material disruption, see Figs. 1(c) and 1(d). This may be the result of a phase explosion:[14,16] at high fluences, the initial energy density in the sample is so high that the thermodynamic cooling path in the phase diagram (e.g., an isentropic cooling, see Ref. 20) takes the system close to the critical point so that the overheated material decomposes spontaneously into a mixture of vapor-phase atoms and liquid droplets.

In order to gain more information about the material swelling, which dominates the structures close to the threshold, the near-threshold bumps have been investigated more thoroughly. Figure 4 shows SEM and AFM images of a bump formed below the threshold for formation of the circular rim. The SEM of the surface, panel (a), shows a roughening, which correlates well with the swollen area, panel (b). The overall shape of the swollen area is reproducible on a shot-to-shot basis, but the precise microstructure varies, reflecting the statistical nature of the process. The microstructure does not reflect hot spots in the laser beam. According to the AFM

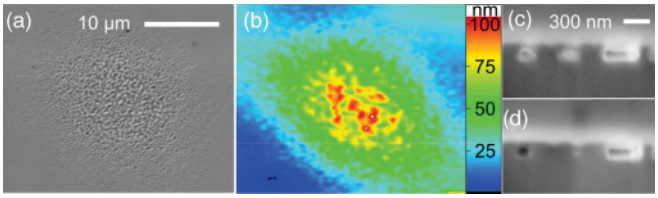

FIG. 4. (Color online) (a) SEM and (b) AFM images of the swelling due to irradiation at low fluence, 0.79 J/cm^2. (c) SEM images (taken at 54° from the surface normal) of the same spot after focused-ion-beam milling. The bottom dark-gray area is the aluminum sample, while the top lighter gray stems from a protective tungsten layer. (d) Same as panel (c) after another 50-nm milling.

image, there is a net height increase, so to determine the origin of this, we have used focused-ion-beam (FIB) milling to obtain a cross section of the sample below the bump. This requires a protective tungsten coating of the sample. The SEM images of the milled sample, panel (c) show the formation of voids below the surface. Some of these appear to have been partially filled by the tungsten, indicating that they are open to the surface. Others, e.g., in panel (d), have clearly been left unfilled. Large-scale images show that the void channels decrease in size when moving radially outwards in the laser beam profile, and eventually diminish below our resolution, explaining the bump in AFM profiles like those shown in Fig. 2.

We have also tried to quantify the swollen features by measuring their diameter and fitting to an expression similar to that used for the clear rims. Since the bumps are not as easy to measure in a consistent way due to absence of a clear boundary, the minor and major spot sizes are fixed to the values obtained from the previous fit to the rim diameters. The bump threshold obtained in this way is (0.7 ± 0.1) J/cm^2.

Let us discuss the mechanisms behind the material response. Microbumps induced by ultrashort pulses have previously been observed for thin metal foils on transparent substrates,[21] and in backside spallation of thin metal films.[22] These phenomena are attributed to photomechanical fracture, where a reflected pressure wave leads to the ejection of a molten phase. They have successfully been modeled by molecular-dynamics (MD) simulations of small material slabs.[23] However, the present results cannot be due to the same phenomena, since the bulk nature of the sample (several millimeter thickness) excludes the influence of a substantial reflected pressure wave.

Instead, a more likely explanation must be based on front-side photomechanical effects. In fact, front-side spallation has recently been predicted by both hydrodynamic simulations,[24] MD modeling,[25] and combined two-temperature and MD modeling.[16,26] The picture is that the short pulse induces a strong pressure wave, which propagates into the material, and it is the combined effect of this pressure and the highly excited material, which leads to material fracture. According to theory, photomechanical material expulsion from the front surface should actually be the dominant ablation mechanism at threshold, although this has not been verified experimentally.

Although the MD simulations reported by Refs. 16 and 26 have been undertaken for Ni, the physical mechanisms for Al should be similar.[27] The swelling observed in the present investigation may thus be coined "frustrated ablation." The morphology of the surface revealed by the cross-sectional measurements shows that the material is not ejected as a single layer. The material seems to freeze in a porous foamy structure with voids of different sizes, which is consistent with the freezing of multiple spalled layers, see e.g., Ref. 16. This freezing is not captured by the MD simulations, which is presumably due to the size of the computation: the lateral size is so small that the appearance of a few voids results in percolation of voids and leads to spallation, a limitation which is enhanced by the typical use of periodic boundary conditions in the MD simulations.[27] The formation of microscopic voids has, however, been seen in MD simulations.[26]

Information about the dynamics of the bump formation can in principle be obtained by time-resolved optical measurements if the geometrical changes and changes to the optical properties can be disentangled. Time-resolved interferometry of an Al surface following excitation by a fluence of 0.75 J/cm^2 (i.e., just above the threshold for bump formation determined in the present investigation) was recently reported.[28] The authors observe a phase shift, which they attribute to a rapidly developing material expansion (∼4 nm at the longest delay time measured, 7 ps). An extension of this work to even longer times would possibly allow measuring the full formation of a bump. At higher fluences, the dynamics of spalled layers may be revealed by the time-evolution of Newton rings, as discussed in Ref. 20.

In order to determine the material dependence of the new observations, we have initiated an investigation of a silver (100) crystal. These investigations, which will be reported in detail elsewhere, exhibit qualitatively the same behavior as a function of the laser fluence. In particular, the bumps at low laser fluence are also observed for the silver target.

The formation of the frozen structures seems to require a stronger cooling mechanism than what is currently incorporated in the theoretical models. Particularly, this cooling must be active after the spalled layers partially loose physical contact to the bulk of the sample. One possible mechanism may be cooling by evaporation of hot atoms[14] and/or hot electron emission,[29] leaving a sample with lower energy density. Another cooling pathway may be cooling through connected material bridges, an effect which may be hard to capture in limited-size simulations. In order to gain more knowledge about the nature of such a cooling mechanism, a control experiment has been undertaken, in which the sample is cleaned in the usual way by sputtering and annealing, but where the UHV chamber is filled to atmospheric pressure by helium before irradiation of the sample. The experiment successfully reproduced the development of the material response, including the formation of bumps. This rules out cooling mechanisms restricted to vacuum conditions.

In general, the thresholds for material modification reported in the present Brief Report are significantly larger than threshold fluences previously reported for aluminum, which are typically in the range of 0.1–0.2 J/cm^2.[11–14] However, contrary to these experiments, the current study investigates the threshold of a single-crystal sample under well-defined conditions. For example, one would expect a lower threshold for a polished sample, which has not been sputtered and annealed as it would have a rougher surface with an amorphous

surface layer. In addition, a common way to determine the threshold is to measure the depth made by hundreds or thousands of pulses, and taking the ablation rate to be an average over pulses, possibly extrapolating to a low number of pulses.[11–13] The threshold measured in this way is presumably lower due to incubation effects. Amoruso *et al.*[14] measured the ablation rate from the number of particles ejected, while in the current paper, ablation is defined as being macroscopic, i.e., material removal, which can be detected by SEM and AFM.

We emphasize that the larger threshold in the present investigation is in fact in good agreement with our simulations of the two-temperature model. The increased threshold is linked to the increased apparent penetration depth, since the energy is redistributed over a larger volume. Note that this increase of both quantities is, in the present work, reproduced by a standard two-temperature model calculation, without the need for inclusion of, e.g., ballistic electron transport. A recent investigation showed that (for multi-pulse irradiation), ballistic electrons were needed to explain the ablation behavior of noble metals, while it played little or no role for tungsten.[15] Aluminum has a strong electron-phonon coupling (like tungsten), which may explain why the effect of ballistic transport is not needed to explain the present data.

In conclusion, we have studied the response of single-crystalline bulk aluminium (111) after irradiation by a single ultrashort near-infrared laser pulse under ultrahigh vacuum conditions. Immediately above the damage threshold, the material exhibited a significant swelling, while substantial material removal required ∼25% larger fluences. The observation is attributed to "frustrated ablation," where the material, which is ejected from the sample by a combination of the high temperature and a strong pressure wave, is frozen in a porous structure with bulk voids. The fact that the same qualitative behavior is observed for silver strongly suggests that material swelling being the first step of ultrashort-pulse laser ablation is a general trend for (single-crystalline) metals.

This work was supported by the Danish Council for Independent Research | Natural Sciences (FNU). We wish to acknowledge the help of J. Rafaelsen, Aalborg University, for assistance with the FIB-SEM imaging and L. Zhigilei, University of Virginia, for fruitful discussions.

*balling@phys.au.dk

[1] K. Sokolowski-Tinten and D. von der Linde, J. Phys. Condens. Matter **16**, R1517 (2004).
[2] B. J. Siwick, J. R. Dwyer, R. E. Jordan, and R. J. D. Miller, Science **302**, 1382 (2003).
[3] W. Kautek and J. Kruger, in *Laser Materials Processing: Industrial and Microelectronics Applications*, edited by E. Beyer *et al.*, Proceedings of the SPIE, Vol. 2207 (SPIE - Int Soc Optical Engineering, Vienna, Austria, 1994), pp. 600–611.
[4] P. Pronko, S. Dutta, J. Squier, J. Rudd, D. Du, and G. Mourou, Opt. Commun. **114**, 106 (1995).
[5] S. Preuss A. Demchuk, and M. Stuke, Appl. Phys. A **61**, 33 (1995).
[6] B. Chichkov, C. Momma, S. Nolte, F. von Alvensleben, and A. Tunnermann, Appl. Phys. A **63**, 109 (1996).
[7] D. Bäuerle, *Laser Processing and Chemistry*, 3rd ed. (Springer-Verlag, Berlin 2000).
[8] S. I. Anisimov, B. L. Kapeliovich, and T. L. Perel'man, Zh. Eksp. Teor. Fiz. **66**, 776 (1974) [JETP **39**, 375 (1974)].
[9] C. Frischkorn and M. Wolf, Chem. Rev. **106**, 4207 (2006).
[10] K. Vestentoft and P. Balling, Appl. Phys. A **84**, 207 (2006).
[11] B. H. Christensen, K. Vestentoft, and P. Balling, Appl. Surf. Sci. **253**, 6347 (2007).
[12] M. K. Kim, T. Takao, Y. Oki, and M. Maeda, Jpn. J. Appl. Phys. **39**, 6277 (2000).
[13] A. E. Wynne and B. C. Stuart, Appl. Phys. A **76**, 373 (2003).
[14] S. Amoruso, R. Bruzzese, M. Vitiello, N. N. Nedialkov, and P. A. Atanasov, J. Appl. Phys **98**, 044907 (2005).
[15] J. Byskov-Nielsen, J.-M. Savolainen, M. S. Christensen, and P. Balling, Appl. Phys. A **103**, 447 (2011).
[16] L. V. Zhigilei, Z. Lin, and D. S. Ivanov, J. Phys. Chem. C **113**, 11892 (2009).
[17] J. Schouborg, M. Kaarup, and P. Balling, J. Phys. Condens. Matter **21**, 265003 (2009).
[18] J. M. Liu, Opt. Lett. **7**, 196 (1982).
[19] Z. Lin, L. V. Zhigilei, and V. Celli, Phys. Rev. B **77**, 075133 (2008).
[20] K. Sokolowski-Tinten, J. Bialkowski, A. Cavalleri, D. von der Linde, A. Oparin, J. Meyer-ter-Vehn, and S. I. Anisimov, Phys. Rev. Lett. **81**, 224 (1998).
[21] F. Korte, J. Koch, and B. N. Chichkov, Appl. Phys. A **79**, 879 (2004).
[22] H. Tamura, T. Kohama, K. Kondo, and M. Yoshida, J. Appl. Phys. **89**, 3520 (2001).
[23] D. S. Ivanov, Z. Lin, B. Rethfeld, G. M. O'Connor, T. J. Glynn, and L. V. Zhigilei, J. Appl. Phys. **107**, 13519 (2010).
[24] M. E. Povarnitsyn, T. E. Itina, M. Sentis, K. V. Khishchenko, and P. R. Levashov, Phys. Rev. B **75**, 235414 (2007).
[25] N. Nedialkov, S. Imamova, P. Atanasov, P. Berger, and F. Dausinger, Appl. Surf. Sci. **247**, 243 (2005).
[26] E. Leveugle, D. S. Ivanov, and L. V. Zhigilei, Appl. Phys. A **79**, 1643 (2004).
[27] L. Zhigilei (private communication).
[28] N. A. Inogamov, V. V. Zhakhovskii, S. I. Ashitkov, V. A. Khokhlov, Y. V. Petrov, P. S. Komarov, M. B. Agranat, S. I. Anisimov, and K. Nishihara, Appl. Surf. Sci. **255**, 9712 (2009).
[29] N. M. Bulgakova, R. Stoian, A. Rosenfeld, I. V. Hertel, and E. E. B. Campbell, Phys. Rev. B **69**, 054102 (2004).